Contour Extraction Using Particle Filters

ChengEn Lu[1], Longin Jan Latecki[2], and Guangxi Zhu[1]

[1] Dept. of Electronics and Info. Eng., Huazhong Univ. of Scie. and Tech., China
[2] Dept. of Computer and Info. Sciences, Temple University, Philadelphia, USA
luchengen@gmail.com, latecki@temple.edu, gxzhu@hust.edu.cn

Abstract. This paper describes a novel approach to extract object region from an image by tracking the enclosing contour. We assume that the image is not complex, and it can be roughly partitioned into two parts with an intensity threshold. A lot of images (for example medical images) are in accord with this assumption. Global constraint (threshold) and local constraint (gradient) are integrated in a particle filter framework. We utilize the filter to track the optimal contour path pixel by pixel. The processing time depends only on the contour length and the number of particles used. Thus the proposed method is significantly faster than the very popular and time consuming method: Active Contour Models ("Snakes"). Both Snakes and our method are targeted for similar applications. Experimental results illustrate the validity and advantages of our method.

1 Introduction

The problem of segmenting an image into meaningful regions is one of the most significant problems in the computer vision area. One of the normal approaches to represent these regions is to use their enclosing contours. Thus, the issue of how to find the enclosing contours of these regions is very critical. Since object detection from cluttered images clearly need prior knowledge (e.g., shape model) of object region, here, we only focus on images with simple intensity distribution. We assume that the background or the foreground of an image has relative homogenous intensity distribution. Actually, a lot of images (such as medical images) are in accord with this assumption. Currently, there are mainly two kinds of methods: region-based methods and edge-based methods.

Region-based methods rely on the homogeneity of spatially localized features such as gray level intensity and other pixel statistics, and they also integrate some edge features such as gradient feature. Region-based methods yield enclosing contours of the regions as simple closed curves, like watershed [1], Active Contour Models [2–5], etc.

Edge-based methods [6–8] primarily utilize gradient operator to locate object boundaries. Gradient information could be based on intensity, color and texture, etc. Gradient operator is a local descriptor, and in most cases we need global constraint to describe the object region. Boundary growing direction is determined by the orthogonal direction of gradient. But, gradient direction is

very sensitive to noise and gradient is ambiguous at corners , e.g., see Fig. 1(a). This is especially dangerous when tracking object contour with a single path, any error can lead to the failure of entire system. Thus, edge-based methods are usually used as edge detectors and they usually do not yield the enclosing object contour without further processing.

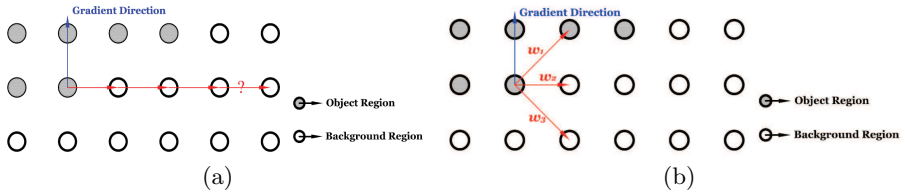

Fig. 1. The difference between single path tracking and multiple path tracking: (a) Tracking with only one path fails at a corner; (b) Multiple paths search for the correct contour point.

The theory of particle filter [9] helps us solve the problem. A significant advantage of particle filter is that it can keep multiple contour hypotheses simultaneously. Each particle is one contour path in our application.

Some efforts have been dedicated to put the edge-extracting method into the framework of particle filter. *Blake* et al [10] first utilized particle filter for contour extraction, but their method only considers local gradient constraint, which makes their method very easy to fail while tracking object boundary (see Fig. 2(b)). In some papers, the prior knowledge of shape model [11–13] is introduced to obtain object region in cluttered background.

This paper combines global and local image constraint smoothly by particle filter and focuses on contour extraction based on low-level knowledge of image. Firstly, benefitting from the homogeneity of the image, we use a global threshold to roughly partition it into two parts. Secondly, we introduce multiple paths at each tracking step with local gradient operator, and use particle filter to find the optimal path (see Fig. 1(b)). In order to be tolerant to noise, we introduce two different scales of gradient operator, one controlling the contour direction, and the other providing local constraint.

Either global constrains or multiple paths can only partly solve the problem of edge-based method. In Fig. 2, we give an example to illustrate that both global intensity threshold in (a), and particle filter without global constraints [10] in (b) cannot process well. But if they are combined together in a proper way, we are able to obtain a correct contour (c).

The combination of global intensity, gradient operator and particle filter is suitable to process the images with homogenous background. Compared to "Snakes", which are widely applied in these images, our method is more efficient. The processing time of the proposed method is only decided by the length

(a) (b) (c)

Fig. 2. (a) Thresholded image; (b) Gradient tracking by [10]; (c) Both methods combined yield a correct result.

of contour and the particle number used, while it is well known that "Snakes" are very time consuming methods.

The rest of the paper is organized as follows. In Section 2, we describe the algorithm in details. Extensive experimental results and comparison with other approaches are presented in Section 3. Finally, the conclusion and discussion is given in Section 4.

2 Algorithm descriptions

The basic structure of our algorithm is similar to the general contour tracking algorithms. That is, first specify a start point, then start the contour tracking process pixel by pixel. When ending condition is satisfied, the tracking process is terminated as illustrated in Fig. 3.

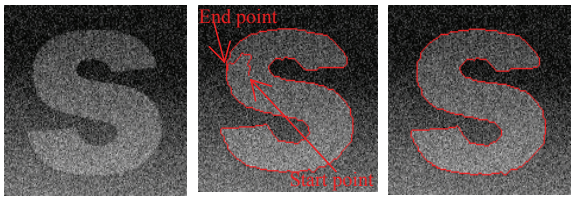

(a) (b) (c)

Fig. 3. An illustration of our approach: (a) Original image; (b) Contour extraction result; (c) Result of removing extra points in (b).

We utilize particle filter to get the optimal contour. The growing contour is represented by an ordered sequence $x_{0:t} \equiv (x_0, \ldots, x_t)$ with the start point x_0. Given the observations $z_{1:t} \equiv (z_1, \ldots, z_t)$, The posterior $p(x_{0:t+1}|z_{1:t})$ can be used to estimate the next contour point x_{t+1}. Contrary to standard tracking problems where data arrives one bit after another as time passes by, the whole set

of data Z is standing there at once in our case. Let $\{x_t^i, \quad i = 0, \cdots, N_s\}$ denote a set of samples or particles and $\{w_t^j, \quad j = 0, \cdots, N_s\}$ denote the associated weights. The weight of a particle at time step t can be approximated as [9]

$$w_t^i \propto \frac{p\left(x_t^i | z_{1:t}\right)}{q\left(x_t^i | z_{1:t}\right)} \tag{1}$$

Rewritten in the form of recursive update formula as:

$$w_t^i \propto w_{t-1}^i \frac{p\left(z_t | x_t^i\right) p\left(x_t^i | x_{t-1}^i\right)}{q\left(x_t^i | x_{t-1}, z_{1:t}\right)} \tag{2}$$

The proposal distribution is usually chosen to be the prior probability [9]

$$q\left(x_t | x_{t-1}, z_{1:t}\right) = p\left(x_t | x_{t-1}\right) \tag{3}$$

Then we get

$$w_t^i \propto w_{t-1}^i p\left(z_t | x_t^i\right) \tag{4}$$

Finally, to avoid the degeneracy of particles, a resampling step is added, which is called Sampling Importance Resampling (SIR) filter [9]. The likelihood

$$p\left(z_t | x_t^i\right) = p_g \cdot p_l \tag{5}$$

is composed by two parts: global p_g and local p_l, which are defined below.

2.1 Global and local constraints

In this paper, we utilize the threshold of global intensity as global constraint. It is easy to get optimal intensity threshold I_o with Ostu's between-class variance method [14], which is described as follow.

In the case of bi-level thresholding of an image, the pixels are divided into two classes, C_1 with gray levels $\{1, \ldots, j\}$ and C_2 with gray levels $\{j+1, \ldots, L\}$. The gray level probability distributions for the two classes are $\omega_1(j)$ and $\omega_2(j)$, and the mean intensities for each class are $\mu_1(j)$ and $\mu_2(j)$. Let u_T indicate mean intensity of the whole image. Then define between-class variance value as:

$$\sigma_B^2(j) = \omega_1(j)\left[\mu_1(j) - \mu_T\right]^2 + \omega_2(j)\left[\mu_2(j) - \mu_T\right]^2 \tag{6}$$

The optimal threshold I_o that maximizes equation (6) is given by:

$$I_o = \arg\max\left(\sigma_B^2\left(j\right)\right) \tag{7}$$

For some images, if the intensity distribution is not simple and the optimal threshold is not easy to obtain, we also can specify the threshold I_o manually.

Global constraint is defined as:

$$p_g\left(x_t^i\right) = \exp \frac{\left(I_{x_t^i} - I_o\right)^2}{2\sigma_I^2} \tag{8}$$

where $I_{x_t^i}$ means the intensity at pixel x_t^i.
Local constraint is generated by gradient defined as:

$$p_l\left(x_t^i\right) = \frac{1}{1 + \left(\lambda / \left\|\nabla(x_t^i, \sigma_L)\right\|\right)^2} \tag{9}$$

Where $\nabla(x_t^i, \sigma_L)$ indicates the gradient at pixel x_t^i, and σ_L indicates the scale of the operator, which is very small in order to guarantee the accuracy of localization. Finally we obtain

$$p\left(z_t | x_t^i\right) = \frac{\exp\left(-\left(I_{x_t^i} - I_o\right)^2 \Big/ 2\sigma_I^2\right)}{1 + \left(\lambda / \left\|\nabla(x_t^i, \sigma_L)\right\|\right)^2} \tag{10}$$

The value of λ serves to characterize the relative strength between p_g and p_l. Essentially the proper value of λ represents good balance between the gradient and intensity information.

The interaction of p_g and p_l can be explained more clearly by the experimental results in Fig. 4, where (a) is the source image, (b) presents the result of Canny operator and (c) provides the thresholded result. It can be seen from (b) that the edge detection resulted from Canny detector includes many disconnected edges, which indicates that it is not easy to extract the object contour by gradient information only. This claim is confirmed by the result in (d). (d) is the result with a constant p_g, which means that only the local gradient constraint p_l takes effect. On the other hand, (e) is the result with a constant p_l, which means that only p_g , i.e., the global threshold constraint is considered. In (e), a rather good outline is obtained from the thresholded image (c). However, the outline is not the actual boundary of the plane. When p_g and p_l are combined in a proper way, we can obtain a significantly better contour as shown in (f).

2.2 Contour direction

At each tracking step, we consider the tracking direction as the three adjacent directions of gradient's orthogonal direction, as Fig. 1(b) illustrates. The orthogonal direction of gradient $\theta_{x_t^i}$ is given by:

$$\theta_{x_t^i} = \arg\max\left((\cos\theta, \sin\theta) \cdot \nabla(x_t^i, \sigma_H)\right)^{\perp} \tag{11}$$

Where $\theta \in \{0, \pi/4, \ldots, 2\pi\}$ means the 8 neighborhood directions of pixel x_t. And $\nabla(x_t^i, \sigma_H)$ is the gradient operator with scale σ_H at pixel x_t^i, which is large enough to guarantee the stability of gradient direction. Then, we get $\theta_{x_t^i}$ as the most proper contour direction. To solve the problem displayed in Fig. 1(a), we introduce multiple paths as Fig. 1(b) illustrates. Instead of one settled tracking path, we consider three directions as candidates: $\Theta_{x_t^i} \equiv \left\{\theta_{x_t^i} - \pi/4, \theta_{x_t^i}, \theta_{x_t^i} + \pi/4\right\}$, which naturally makes the proposal distribution:

$$p\left(x_{t+1}^i | x_t^i\right) \propto \begin{cases} 1 & x_{t+1}^i \in N(x_t^i, \Theta_{x_t^i}) \\ \epsilon & x_{t+1}^i \notin N(x_t^i, \Theta_{x_t^i}) \end{cases} \tag{12}$$

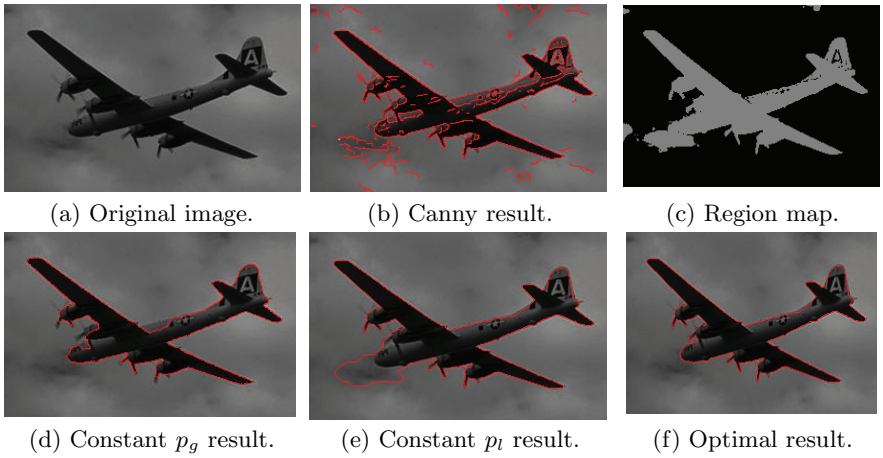

(a) Original image. (b) Canny result. (c) Region map.

(d) Constant p_g result. (e) Constant p_l result. (f) Optimal result.

Fig. 4. Performance of our algorithm with various parameters. The results of our algorithm are shown in (d) to (f). (d) is the result by fixing the global constraint p_g, and only the local gradient constraint is considered; (e) is the result by fixing the local constraint p_l, and only the global threshold constraint is considered; In (f), we consider both constraints, and then a better contour is extracted.

where $N(x_t^i, \Theta_{x_t^i})$ means the neighbor pixels of x_t^i with direction belonging to $\Theta_{x_t^i}$ and ϵ is a very small constant.

2.3 Starting and ending conditions

The start point can be chosen as the pixel that maximizes equation (10). In some cases where the intensity distribution is very complex, we still need to choose the start point manually. Once a tracking path forms a closed contour, the contour sequence is long enough, and the corresponding particle owns the highest weight, we end the tracking processing and the path is selected as the final contour path.

2.4 Summary

Initialize N particles with the weights $w_0^1, w_0^2, \ldots, w_0^N$ equal to $1/N$. To maintain the diversity of contour paths, in the intermediate process we always keep N particles, and each particle represents an independent contour path. From the "old" sample set $\{(x_{t-1}^i, w_{t-1}^i) \quad i = 1, \ldots, N\}$ at time $t-1$, construct a new sample set $\{(x_t^i, w_t^i) \quad i = 1, \quad \ldots, N\}$ for time t. The procedure is as follow:

- *while*(1)
  - *for* $i = 1$ to N
    - ∗ **Prediction by Sampling:** extend each particle to three particles, $x_{1:t}^k = \{x_{1:t-1}^i, x_t^k\}$, where $x_t^k \in N(x_{t-1}^i, \Theta_{t-1}^i)$.

∗ **Importance Weighting:** Compute weights: $w_t^k = p(z_t|x_t^k)w_{t-1}^i$.

- end of *for*
- **Subsampling:** Draw N particles from current set of $3N$ particles by Sampling Importance Resampling (SIR) filter [9].
- if(ending condition is satisfied(see section: 2.3)) exit(*while*).
- normalize weights: $\sum_i^N w_t^i = 1$ and update status: $t \leftarrow t+1$.

– end of *while*

3 Experimental results

3.1 Comparison with JetStream [10]

The results in Fig. 5 are the comparisons between JetStream [10] and our approach. In some images (image: "elephant", "plane" and "running woman"), the start point and intensity threshold are manually specified for the proposed method. There is no human interaction for both methods once the tracking process starts. It is obvious that the proposed approach is able to generate better results than JetStream in these applications, which proves the effect of global constrains.

(a) Original image.

(b) JetStream results.

(c) Our algorithm results.

Fig. 5. Comparisons with JetStream. Our algorithm have better performance for images with homogenous background(image: "hand", "plane", "toy" and "ice crystal").

3.2 Contour extraction from noisy images

Comparison experiments to examine the respective tolerance to noise of our algorithm and several popular Active Contour Model ("Snake") methods are given in Fig. 6. Impulse noise is added to the original image with intensity varying from 10% to 60%, as shown in Fig. 6(a). Fig. 6(b) to (d) provide the segmentation results of the standard Snake, GGVF [4] and RAGS [5] respectively. Fig. 6(e) shows the results of the proposed approach. The comparison illustrates the proposed approach can track the correct contour from noisy images, which is more robust than the other three methods.

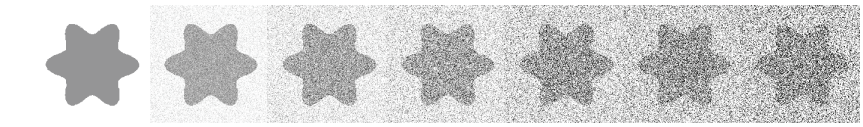

(a) Original image with various levels of added Gaussian noise [0%, 10%,. . . ,60%].

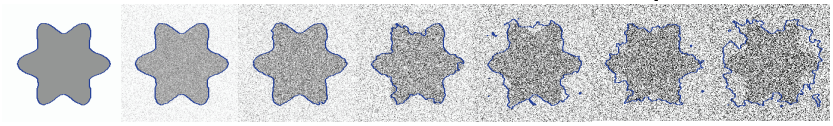

(b) Standard geometric snake results.

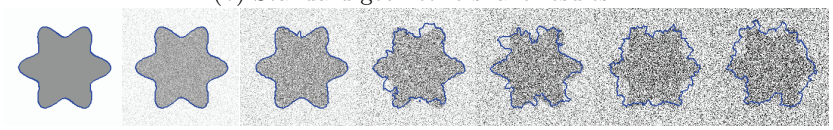

(c) GGVF snake results.

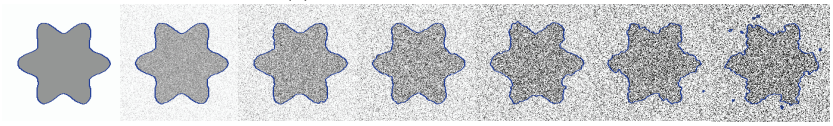

(d) RAGS snake results.

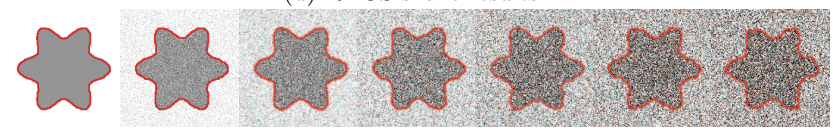

(e) Our algorithm results.

Fig. 6. Shape recovery from noisy images.

3.3 Results from images with intensity inhomogeneous background

To further test the performance of the proposed approach, we perform several experiments for intensity-inhomogeneous images, in comparison with the other

two algorithms of "snakes" type, namely PS model [2] and LBF model [3], both of which are suited to the above images. This kind of intensity-inhomogeneity widely exists in medical images. From the results shown in Fig. 7((a) and (b) are quoted from [3]), it can be seen that our algorithms have comparable performance with the other two algorithms, while our approach takes much less processing time, as shown in Table 1 . A few more results of our method on actual medical images can be found in Fig. 8.

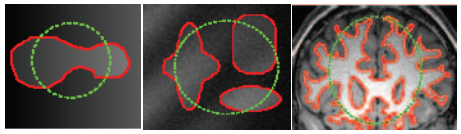

(a)LBF model [3] results.

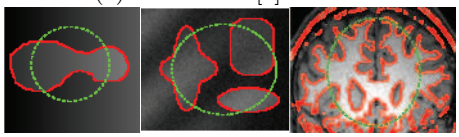

(b)PS model [2] results.

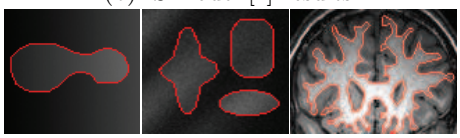

(c)Our algorithm results.

Fig. 7. Results from images with intensity inhomogeneity background.

Table 1. Comparison of time consumption (in sec.) with 2.8G CPU computer.

	Image 1	Image 2	Image 3
LBF Model	1.78	2.42	11.85
PS Model	39.92	101.89	203.03
Our Algorithm	**0.02**	**0.05**	**4.23**

4 Conclusion and future work

This paper presents a novel edge-based image segmentation algorithm using the framework of particle filter. We combine gradient operators of two scales and global threshold constraint to guarantee the robustness and accuracy of edge

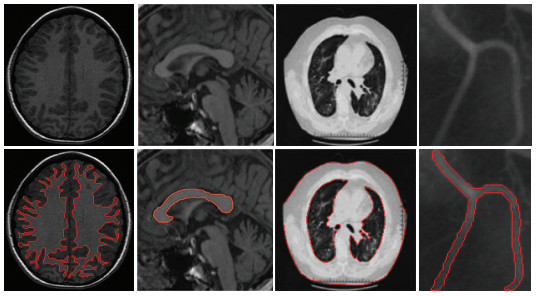

Fig. 8. More results on medical images.

locating. The proposed method has very comparable performance with the popular method "Snakes", and our method shows the advantage of less processing time. In addition, this algorithm can be extended to contour extraction based on high-level knowledge, which we plan to incorporate in our future work.

References

1. Vincent, L., Soille, P.: Watersheds in digital spaces - an efficient algorithm based on immersion simulations. PAMI **13** (1991) 583–598
2. Vese, L., Chan, T.: A multiphase level set framework for image segmentation using the mumford and shah model. Int'l J. Comp. Vis. **50** (2002) 271–293
3. Li, C., Kao, C.Y., Gore, J.C., Ding, Z.: Implicit active contours driven by local binary fitting energy. CVPR (2007)
4. Xu, C., Prince, Jerry, L.: Generalized gradient vector flow external forces for active contours. Signal Process **71** (1998) 131–139
5. Xie, X., Mirmehdi, M.: Rags: Region-aided geometric snake. IEEE Transactions on Image Processing **13** (2004) 640–652
6. Canny, J.: A computational approach to edge detection. PAMI **8** (1986) 679–698
7. Martin, D.R., Fowlkes, C.C., Malik, J.: Learning to detect natural image boundaries using local brightness, color, and texture cues. PAMI **26** (2004) 530–549
8. Dollar, P., Tu, Z., Belongie, S.: Supervised learning of edges and object boundaries. CVPR (2006)
9. Arulampalam, S., Maskell, S., Gordon, N., Clapp, T.: A tutorial on particle filters for on-line non-linear/non-gaussian bayesian tracking. IEEE Trans. Signal Processing **50** (2002) 174–188
10. Prez, P., Blake, A., Gangnet, M.: Jetstream: Probabilistic contour extraction with particles. ICCV (2001) 524–531
11. Zhang, J., Collins, R., Liu, Y.: Representation and matching of articulated shapes. CVPR **2** (2004) 342–349
12. Fan, X., Qi, C., Liang, D., Huang, H.: Probabilistic contour extraction using hierarchical shape representation. ICCV **1** (2005) 302–308
13. Bai, X., Yang, X.W., Latecki, L.J.: Detection and recognition of contour parts based on shape similarity. Pattern Recognition **41** (2008) 2189–2199
14. Ostu, N.: A threshold selection method from gray-level histogram. IEEE Transactions on System Man Cybernetics **9** (1979) 62–66